TD-01-061
08/01

Fermi National Accelerator Laboratory
Technical Division / Development & Test Dept.
PO Box 500 MS 316
Batavia, IL 60510
FAX : 630-840-2383

SYNCHROTRON RADIATION ISSUES IN FUTURE LARGE HADRON COLLIDERS

Summary of contributions to the T2 WG at the Snowmass 2001 conference

P. Bauer, C. Darve, I. Terechkine

Abstract:

Ever since a post LHC hadron collider is being discussed, synchrotron radiation was identified as a major technological issue. The synchrotron radiation power emitted by the protons, scales with the fourth power of the particle energy. Therefore, any energy frontier hadron collider of the future is likely to produce several W/m/beam of synchrotron radiation power. The currently proposed VLHC in its second stage, for example, would produce 5 W/m/beam of synchrotron radiation power. The following discusses the implications of synchrotron radiation and the possible solutions to the problem of extracting the radiation power (most likely from a cryogenic environment) in the range of radiation powers of 1-30 W/m/beam, most likely to occur in the next generation hadron collider.

1.0 INTRODUCTION

Ever since a post LHC hadron collider is being discussed, synchrotron radiation was identified as one of the major technological challenges. The synchrotron radiation power emitted by the protons, scales with the fourth power of particle energy (γ^4), the beam current and ρ^{-2}, where ρ is the arc-bending radius of the machine. Therefore, any energy frontier hadron collider of the future, using high field magnets (to reduce the tunnel size), is likely to produce several W/m/beam of synchrotron radiation power. The currently proposed VLHC in its second stage, for example, would produce 5 W/m/beam of synchrotron radiation power [1]. This level of radiation power is still far below the level of SR in what is believed to be the last circular electron machine, Cern's LEP, which generates ~400 W/m/beam. It is possible to imagine hadron collider scenarios, using very high field magnets and accelerating hadrons to extreme energies, such that similar levels of radiation power arise. However, given the technical limitations in magnet technology, limitations related to the cost of the machine and other limitations (such as beam-energy and IR debris power), a more realistic range of radiation powers of 1-30 W/m/beam is most likely to occur in the next generation hadron collider. The following discusses the implications of synchrotron radiation and the possible solutions to the problem of extracting the radiation power (most likely from a cryogenic environment) in this range of radiation powers.

2.0 SYNCHROTRON RADIATION POWER

Figure 1 shows the calculated SR power level versus machine size (or more precisely the particle trajectory bend radius in the guide field) for various particle energies that are possible in a future VLHC (here assuming an average beam-current I_b=100 mA). The SR power ps_R can be calculated with (1) from Sand's constant C_γ, the proton energy E_b, the beam current I_b and the bending radius of the particle trajectory ρ.

$$p_{SR} = \frac{C_g}{2p}\frac{E_p^4 I_b}{r^2} \quad \left(\frac{W}{m}\right) \tag{1}$$

The presently known solutions to the problem of extracting the SR related heat load from a cryogenic environment, e.g. with a cooled beam-screen or a photon-stop, have their limitations. The following attempts to explore these solutions in the full range of SR heat loads indicated in the introduction. Schematics of the solutions are shown in Figure 2. Two possible beam-screen configurations are shown: A cooled beam-screen, much like the LHC beam-screen and a room temperature beam-screen with an additional screen.

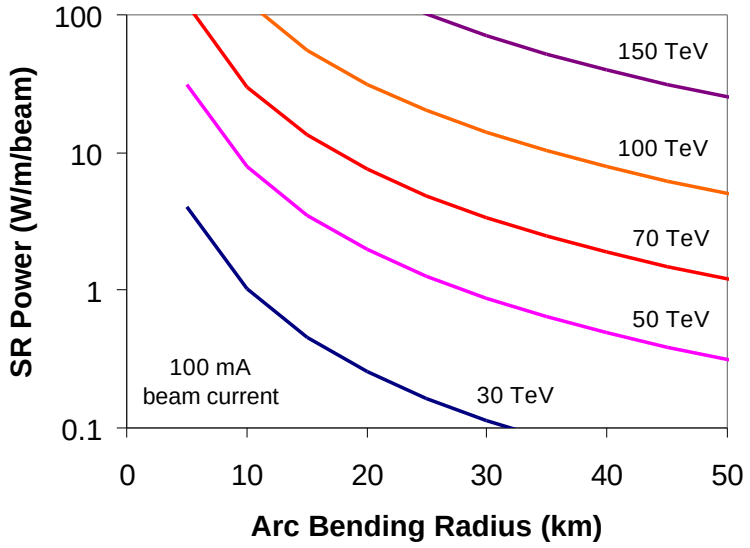

Figure 1: Synchrotron radiation power as a function of arc bending radius for different particle energies and constant beam current (100 mA).

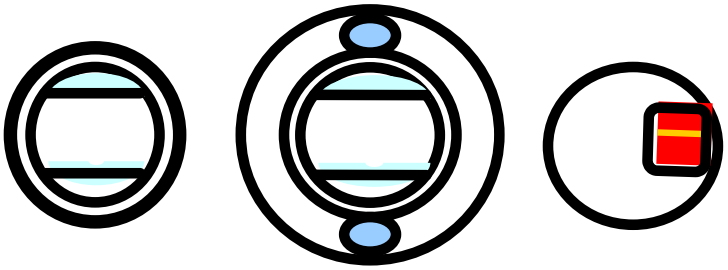

Figure 2: Schematics of different solutions to the SR problem in cryogenic colliders: cooled beam-screen, room temperature beam-screen with internal shield and photon-stop.

2.1 Beam-Screens

The beam-screen solution will look different according to the SR heat load. For a heat load < 10 W/m/beam, a cooled beam-screen - similar to the LHC BS - is a possible solution. To minimize the cryo-power requirements the beam-screen operational temperature has to be raised with increased SR heat load, together with the required He mass flow rate and thus the cooling channel size. Another possible beam-screen solution consists of a room temperature, water-cooled beam-screen surrounded by an 80 K (helium-cooled) shield. The room temperature beam-screen is not attractive at a SR heat load <5 W/m/beam, because it produces a residual heat load of 3.7 W/m/beam (extracted by the "internal" shield placed between the screen and the cold bore), independently of the SR load. In terms of power cost the room temperature beam-screen is the better solution above a SR heat load of 5 W/m/beam. Figure 3 shows the power-cost at the plug per meter per beam for both solutions. The formulas (2), used in these calculations are 2nd

order polynomial fits to numerical calculations presented in detail in [2], [3]. The constants used in the fits are listed in Table 1. The calculations on which fit (2) is based assume 20 bar gaseous helium as the cooling agent, a 135 m length for the cooling loop, a 20 K / 1 bar temperature / pressure drop along the cooling loop, coefficients of conductive and radiative heat transfer between the screen and the cold mass measured at Cern in the frame of the LHC beam-screen development, and operation at the thermodynamically optimal temperature. The optimal temperature rises quickly with increased SR load and reaches ~100 K at ~5 W/m before, saturating at ~120 K at ~20 W/m. Above that load an increase of beam-screen temperature is not favored, because the heat transfer from the screen to the 5 K cold mass becomes prohibitively large. The saturation of the optimal temperature is an indication that an additional shield is required, such as in the case of the room temperature beam-screen.

$$p_{plug} = ap_{SR}^2 + bp_{SR} + c \quad \left(\frac{W}{m}\right) \tag{2}$$

Table 1: Constants of polynomial fit of plug-power requirement of different beam-screen solutions.

	a	*b*	*c*
cooled beam-screen	-0.1503	11.324	7.4119
room-temperature beam-screen	0	1	37.06

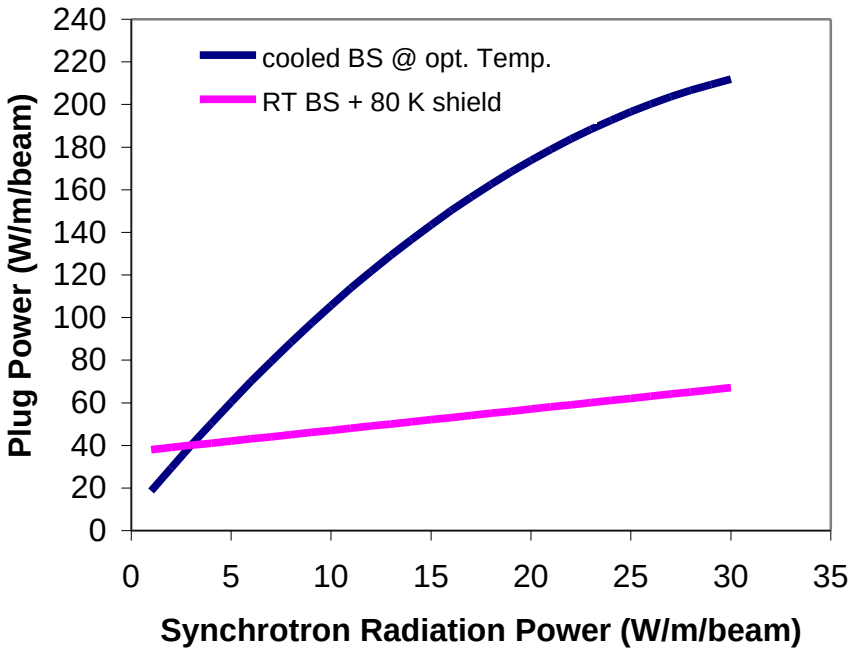

Figure 3: Calculated plug Power for cooled and room temperature beam-screen, per m of machine, per beam. The calculation includes only the heat load on the beam screen (at the Carnot efficiency related to its operating temperature) and the conductive and radiative heat transfer to the cold-mass (which depends as well on the operating temperature).

Although the room-temperature beam-screen solution may appear more attractive at a SR load exceeding 5 W/m, it is not. The room-temperature beam-screen solution requires a larger magnet aperture because of the internal 80 K shield, which makes it un-attractive compared to the more compact cooled beam screen solution. On the other hand, as mentioned above, the cooling channel size requirement in the case of the cooled beam-screen increases with increasing heat load. Therefore, the room temperature beam-screen solution starts to become interesting at a SR power load at which the cooled beam-screen becomes larger than the room temperature beam-screen (whose size is in first approximation SR load independent). It has to be noted as well that the room temperature beam screen creates an engineering problem because the intermittent screen interferes with the cryo-pump function of the cold bore. Figure 4 shows the result of a calculation of the required aperture for the beam-screen solutions as a function of SR heat load. As can be seen in this plot the crossing occurs at ~20 W/m/beam. The calculations on which Figure 4 is based are described in the following. The aperture requirement is estimated from the sum of the equivalent diameters of the various components. First, the minimum beam area assumed in these calculations is a circle with Ø 20 mm. Then, the equivalent diameters of the cold-bore wall, the insertion gap, the cooling tube wall and the support ring are calculated from their respective thickness (multiplying the thickness by 2). The equivalent diameter of the required coolant flux as a function of SR power is calculated with a fit to numerical data presented in [2]. In the case of the RT beam-screen the size of the screen cooling channels and the 80 K shield are assumed to be constant. The additional internal shield in this case requires a second set of gaps and supports which is factored into (4) by doubling the $d_{gap/support}$ and d_{ctwall} contributions.

$$d_{BS} = d_{beam} + d_{ctwall} + d_{cb} + d_{gap/\sup port} + \frac{0.004}{p}\sqrt{17.858\,p_{SR} + 0.34} \quad (m) \tag{3}$$

$$d_{RTBS} = d_{beam} + 2d_{ctwall} + d_{cb} + 2d_{gap/\sup port} + d_{shield} + d_{cool} \quad (m) \tag{4}$$

Table 2: Equivalent diameters (in mm) of various components of the cooled beam-screen (BS) and the room temperature beam screen (RTBS).

beam screen	beam area d_{beam}	cooling tube wall d_{ctwall}	cold-bore wall d_{cb}	gap +supports $d_{gap/support}$	80 K shield d_{shield}	coolant surface d_{cool}
cooled BS	20	3	3	2	-	see (3)
RT BS	20	3	3	2	13	5.3

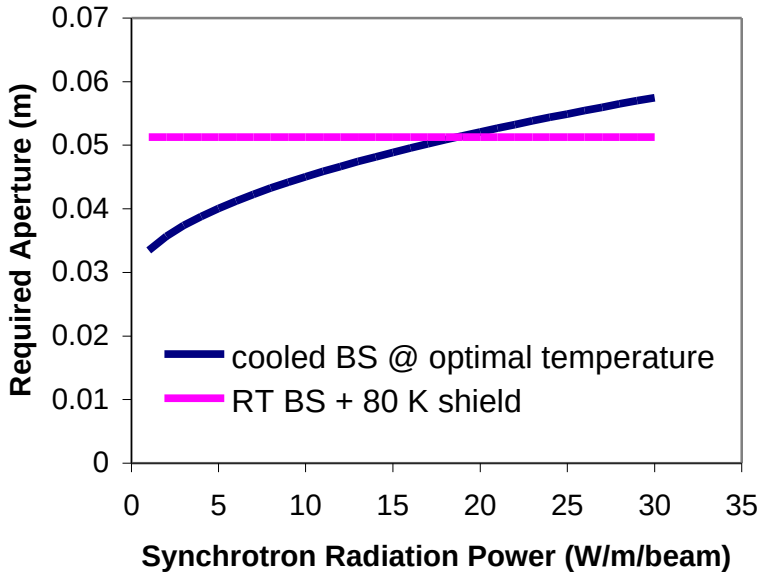

Figure 4: Aperture requirements for the cooled BS and RT-BS as a function of SR heat load.

However, all beam-screen solutions, especially in a large ring, entail large cryo-power requirements and cost. The SR power load in these plots was therefore restricted to ~30 W/m/beam. The cryo-power cost and especially the cost of the enlarged magnet aperture are considerable. The enlarged aperture can be avoided in magnet designs, which have larger vertical apertures (e.g. block-type coils) without increasing the horizontal aperture and thus at no additional cost, where large cooling capillaries can be accommodated. However, such magnets have not been developed yet.

2.2 Photon-Stops

Photon-stops are water-cooled fingers, placed after every bending magnet, that can be driven toward the magnet axis during the magnet ramp to intercept the rising synchrotron radiation power emitted by the accelerated beam. The photon-stop will always be the preferred solution (compared to a beam-screen), because it extracts the SR heat load at room temperature and thus at optimal Carnot efficiency. Unfortunately it remains to be proven that it works. Critical issues of the photon-stop design are primarily related to the surface power-density and secondarily to its impedance. Photon-absorbers in 3rd generation light sources operate at power rates of up to 10 kW, or surface densities up to 1 kW/cm^2. This SR power level certainly exceeds that of any possible future large hadron collider. To restrict the surface power density on the photon-stop, its size has to increase with increasing SR heat load. There seems to be no reason (except space limitations in the magnet interconnect) why such a photon-stop could not be shaped like a wedge (or taper) with a longitudinal extension of up to 1 m. The recent VLHC study [1] has shown that the impedance of a 3.5 cm long photon-stop with 1 cm radial and azimuthal extension is small and the impedance decreases with its length. There is no need to

extend the stop azimuthaly (which would raise the impedance) because the SR light hits it along a very thin line. The impedance of the photon-stop increases roughly with the third power of the radial extension and it should thus not exceed ~2/3 of the beam-tube radius. Under these precautions, we believe, that a photon-stop will be found in all future hadron colliders. However, there are "hard" limits to the applicability of such a device, which are neither related to the thermal requirements, nor to the impedance. They are of geometrical nature and related to the size of the ring and the magnet length and aperture. Photon-stops are only practical in machines with a large enough aperture and a large enough ring. Figure 5 gives a sketch of the SR beams along a set of two magnets. The magnets are assumed to be straight and they are centered with respect to the beam. Furthermore the following calculations assume that the radiation is entirely absorbed in the photon-stops. A magnet rotates the particle velocity vector by Ψ, the opening angle of the trajectory segment covered by one magnet. Ψ is given by the magnet length divided by the arc bending radius R. The plot is based on a “N-2 scheme” in which the photon-stop extracts all the SR from the second magnet up-stream (see Figure 5). The formula for the maximum magnet length can be derived easily from the plot, with r the magnet bore radius, L_s the interconnect (IC) length (here assumed to be 3 m) and the arc bending radius R (5&6).

$$L_m^{\max} \Rightarrow r = L_m \frac{\Psi}{2} + L_s \Psi + \frac{3}{2} L_m \Psi \quad \Psi = \frac{L_m}{R} \quad (m) \tag{5}$$

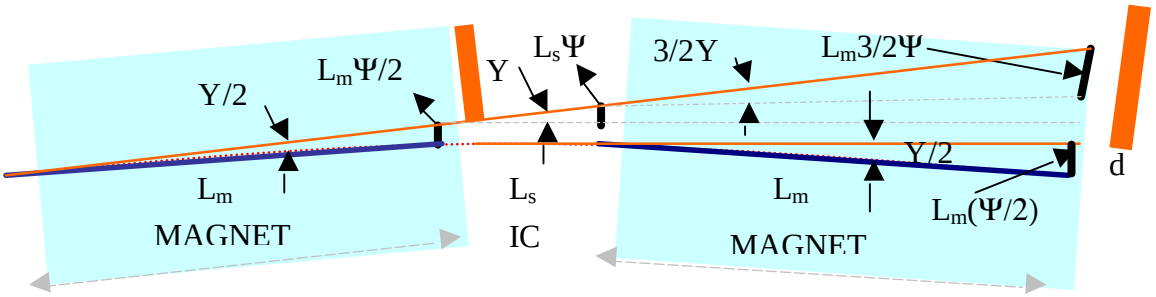

Figure 5: Schematic (top-) view of the particle and SR beam trajectories.

$$L_m^{\max} \approx \sqrt{\frac{rR}{2}} - \frac{L_s}{4} \quad (m) \tag{6}$$

Figure 6 shows the maximum magnet length compatible with photon-stops placed between the magnets (in a 3 m long interconnect section) as a function of machine arc bending radius, for various magnet apertures in the range 20 – 60 mm, as calculated with (6).
The distance d between the tip of the photon-stop and the center of the magnet (where the beam is) can be found with (7):

$$d = L_s \frac{\Psi}{2} + L_m \frac{\Psi}{2} = \frac{L_s L_m}{2R} + \frac{L_m^2}{2R} \quad (m) \tag{7}$$

In (7) the distance d is independent of the constraint on magnet length given by (6). In order to include this constraint the magnet length L_m in (7) can be replaced by L_m^{max} (6) and d^{max} becomes:

$$d^{\max} \approx \frac{r}{4} + \frac{1}{4} L_s \sqrt{\frac{r}{2R}} \quad (m) \tag{8}$$

The scheme shown in Figure 5 allows for a maximum distance d between the photon-stop tip and the beam. Another scheme, in which the photon-stop extracts a $(1\text{-}X)^{th}$ part of the SR from the second magnet up-stream and a $|(X\text{-}1)|^{th}$ fraction of the SR from the first magnet up-stream is discussed in the following. In this "X-scheme", the photon-stop comes closer to the beam, increasing its impedance as well as the risk of accidental beam impact. On the other hand the "X-schemes" allow to use photon-stops in rings with a smaller bending radius than those compatible with the "N-2" scheme. The maximum possible magnet length can again be found from the condition that the radiation emitted at $(1\text{-}X)L_m$ of the second magnet up-stream hits the beam tube wall (radius r) at the end of the next magnet (10). (10) can be resolved in terms of the maximum possible magnet length (11).

$$r = (1-X) L_m \frac{\Psi}{2} + L_s \Psi + \frac{3}{2} L_m \Psi \quad (m) \tag{10}$$

$$L_m^{\max} \approx \sqrt{\frac{2rR}{(4-X)}} - \frac{L_s}{(4-X)} \quad (m) \tag{11}$$

The distance d from the beam is:

$$d = (1-X) \frac{L_m^2}{2R} \quad (m) \tag{12}$$

In a procedure similar to that in the "N-2 scheme", the magnet length L_m in (12) can be constrained through (11), yielding:

$$d^{\max} = \frac{(1-X)}{(4-X)} r - \frac{(1-X)\sqrt{2}}{(4-X)^{3/2}} \sqrt{\frac{r}{R}} L_s \quad (m) \tag{13}$$

As can be easily shown with (13) the distance between the photon-stop and the beam becomes zero whenever X=1.

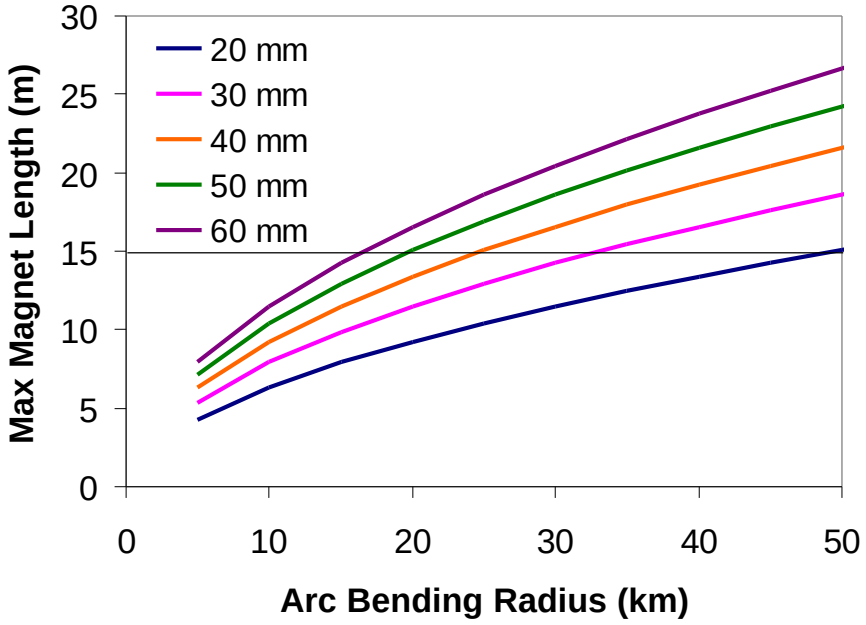

Figure 6: Maximum magnet length compatible with photon-stops versus arc bending radius, for the "N-2 scheme".

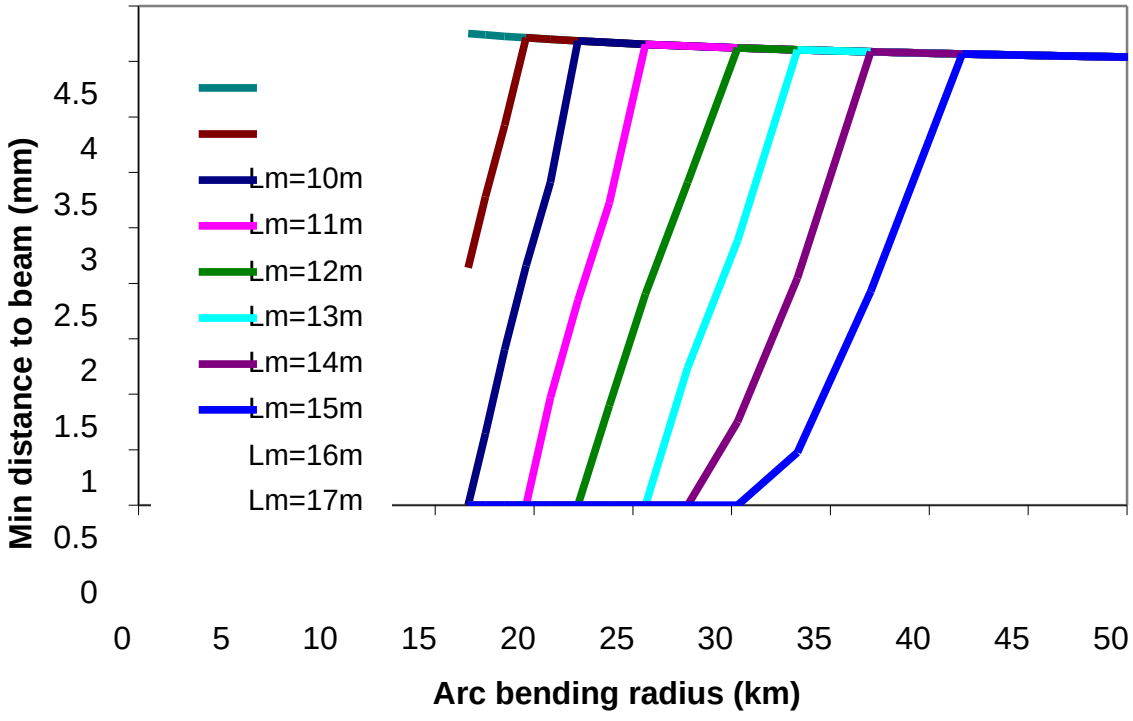

Figure 7: Minimum distance of photon-stop to beam as a function of arc bending radius for a 30 mm physical beam tube aperture and different magnet lengths.

Figure 6 shows the maximum magnet length for different magnet apertures as calculated with (6). As mentioned before a "mixed scheme", would allow to raise the maximum magnet length above the limits indicated in the figure in small bending radius machines. However, since the constraint in this scheme comes less from the magnet length condition, but the distance d to the beam, it is the latter issue that will be discussed next. Figure 7 shows the minimum distance of the photon-stop tip to the magnet axis (and thus the beam orbit) as a function of arc bending radius for a fixed magnet length and aperture (30 mm). The distance d is almost flat in larger machines, which can use the "N-2 scheme". Below the limiting bend radius of the "N-2 scheme" the "X-scheme" is used, which leads to a rapid decrease of the minimum distance as the X-fraction becomes larger. Eventually the bend radius is small enough for the distance to become zero. It is not clear at that point what the minimum acceptable distance between photon-stop tip and beam orbit is. However, a few mm are certainly required.
Furthermore a scheme suggested by Talman [4], in which the magnet is displaced horizontally with respect to the beam orbit, would allow to gain some more mm in separation between the photon-stop and the beam. This scheme has not been addressed in detail here.

Although not confirmed yet, it is almost certain that some pumping mechanism has to be provided together with the photon-stop, as it is for example commonly done in light sources. In a cryogenic machine it would be most reasonable to use the cryo-pump constituted by the cold bore, which is most efficient in conjunction with a (warmer) liner. Therefore, in the current VLHC, it was deemed most prudent to propose a combined solution of beam-screen and photon-stop [1]. In the case, in which the photon-stop is working at full capacity, the beam-screen only fulfills the pump function. In this case the screen could be restricted to the location of the photon-stop only. Another issue worth mentioning in this context, is the engineering design, which for increased SR power becomes more difficult. For example, the thermal radiation power from the room temperature photon-stop surface is 0.17 W for a 10 cm^2 surface.

3.0 CONCLUSIONS

Unlike in most of the electron machines, proton machines use high field superconducting magnets operating at low temperatures. Therefore the issue of extracting a synchrotron radiation power heat load becomes more critical and costly. Solutions to the problem of extracting the synchrotron radiation power heat load exist, namely beam screens and photon-stops. Cooled beam-screens such as in the LHC are not only much more expensive in production and operation than a photon-stop solution, but almost certainly become unattractive above a SR load of 30 W/m/beam. Photon-stops are the most economical solution because the heat load is extracted at room temperature. On the other hand there are (geometrical) limitations to the use of photon-stops, related to the magnet size, magnet aperture and bending radius of the particle trajectory. We are nevertheless confident, that, inspired by the experience with electron colliders and light sources, photon-stops will be an attractive solution to the synchrotron radiation problem in future hadron machines, even for radiation levels similar to those currently found in the most powerful electron machines. We should be even more confident, since proton machines have the undeniable advantage over accelerators of lighter particles, that the larger mass of the protons results in stiffer beams that are less affected by perturbations such as

photon-stops. The limiting parameter for the use of photon-stops is the circumference of the machine (and in relation to it the magnet aperture). Given the (current) limitations in magnet technology to <15 T, such an impediment is not of importance in very large energy rings (> 200 TeV cm), which automatically require a large circumference to allow steering of the beams with the limited magnet technology. An increase of aperture, allowing the use of photon-stops as well in rings of smaller size and energy (e.g. below the current proposal for the VLHC in its second stage), is not a recommendable option since it is uneconomical. Therefore a number of schemes that would allow the use of photon-stops as well in smaller machines were discussed here.

Other effects of SR include photo-induced gas-desorption from the PS or beam-tube walls and radiation damping. Increased particle energy and SR (flux and characteristic energy) seem to have only minor effects on the vacuum system and they are mostly of the facilitating kind. For example, larger SR flux and higher characteristic energy reduce the conditioning time. Due to the increase in proton-residual gas cross-section the vacuum quality has to be raised as one goes toward higher proton-energies, but the effect is small. The big advantage of synchrotron radiation damping allows a considerable gain in luminosity and is believed to be the major advantage of a synchrotron radiation dominated machine.

REFERENCES

[1] P. Limon et al., “VLHC Feasibility Study 2001”, at www.vlhc.org;

[2] C. Darve et al., “VLHC beam-screen cooling”, Fermilab Technical Division Note TD-01-005, Feb. 2001;

[3] P. Bauer et al., “Synchrotron Radiation Issues in the VLHC-2”, published the PAC 2001, Chicago, June 2001;

[4] R. Talman, “Synchrotron Radiation Masks for High Energy Proton Accelerators”, Proceedings of the Future Hadron Facilities Workshop, Bloomington, Indiana, July 1994;